

Direct torque control for an autonomous photovoltaic system with MPPT control

A. Mohammadi¹, D. Rekioua^{1*}

¹Laboratoire LTII, Faculté de Technologie, Université de Bejaia, 06000 Bejaia, Algérie

Received: 27 September 2020; Revised: 27 October 2020; Accepted: 27 November 2020; Published: 30 December 2020

Turk J Electrom Energ Vol.: 5 No: 2 Page: 48-55 (2020)

SLOI: <http://www.sloi.org/>

*Correspondance E-mail: dja_rekioua@yahoo.fr

ABSTRACT This work deals with the control of a photovoltaic pumping system. It is based on an induction motor, and direct torque control (DTC) is applied. The method adopted is based on the instantaneous space vector theory. By optimal selection of the space voltage vectors in each sampling period, DTC archives effective control of the stator flux and torque. The most important advantage of this method is its rotor position free control system. To improve photovoltaic (PV) system performances, Perturb & Observe maximum power point tracking (MPPT) algorithm has been used to achieve sufficient power to operate the water pumping system under variable conditions. Through this work, it is aimed to obtain a simple and low-cost system for the photovoltaic water pumping systems with rapid tracking of the maximum power. The proposed system with DTC and MPPT strategy not only improves system performance but also extends the working hours of solar photovoltaic systems. Simulation of the adopted method is also presented.

Keywords: Photovoltaic, Water Pumping, Direct Torque Control, Maximum power point tracking

Cite this article: A. Mohammadi, D. Rekioua, Direct torque control for an autonomous photovoltaic system with MPPT control, *Turkish Journal of Electromechanics & Energy*, 5(2), 48-55, (2020).

1. INTRODUCTION

The output power induced in the photovoltaic modules depends on climatic conditions [1-3]. To maximize power, several MPPT algorithms have been used [4-18]. The most used control consists to act on the duty cycle automatically to place the generator at its optimal value whatever the variations of the metrological conditions or sudden changes in loads. To track the maximum power point (MPP), a look-up table on a microcomputer is employed by Ramli et al [4]. It is based on the use of a database that includes parameters and data such as typical curves of the PV generator for different irradiances and temperatures. In the curve-fitting method, the nonlinear characteristic of the PV generator is modeled using mathematical equations or numerical approximations. These two algorithms have a disadvantage that they may require a large memory capacity, for calculation of the mathematical formulations and storage of the data. The open-circuit voltage photovoltaic generator method is employed by Karami et al [5]. It approximates linearly the voltage of PV generator at the MPP to its open-circuit voltage and a linear dependency between the current at the MPP and the short-circuit current for the short circuit photovoltaic generator method presented by Reisi et al [6]. These methods are simple and economical, but they are not able to adapt to changeable environmental conditions [7-9].

Presented perturb and observe (P&O) algorithm which is based on iterative algorithms to track continuously the MPP through the current and voltage measurement of the PV module. Most control schemes use the P&O technique because it is easy to implement, but the oscillation problem is unavoidable [10]. The conductance incremental algorithm named as "IncCond" presented by Ghayed et al [11] requires a complex control circuit. The two last strategies have some disadvantages such as; high cost, complexity, and instability. Also, intelligent algorithms based on control by MPPT were introduced [12-18]. The fuzzy logic controller (FLC) optimizes the magnitude of the increment to obtain fast and fine tracking [10]. In sliding mode controller (SMC), the control circuit adjusts the duty cycle of the switch control waveform to obtain MPPT as a function of the evolution of the power input at the DC/DC converter. Neuro-fuzzy systems are fuzzy systems based on the theory of neural networks algorithm (ANN). The learning technique operates according to the local information and produces only local changes in the fuzzy system origin. If the MPPT algorithm performances must be optimal, even for a complex implementation, the choice will be relatively focused on advanced algorithms. If the implementation simplicity is preferred, the choice will be based on classical algorithms [4-8].

The control of induction motors has gained a lot of attention both in academia and industry, recently. One of the most significant developments in this area has been the field-oriented control where partial feedback linearization, together with a proportional-integral. This technique is very useful even though it is very sensitive to parameter variations such as rotor time constant and incorrect flux measurement or estimation at low speeds. DTC for induction machines (IM) is a robustness control method for motor drives. It provides a better solution to improve motor characteristics and the voltage inverter source [19-20]. In principle, the DTC method is performed with the instantaneous space vector theory. Thus, the number of space voltage vectors and switching frequency directly influence the performance of the DTC control system.

In this work, a DTC-IG system of a photovoltaic system is proposed. An application has been performed for water pumping. The P&O MPPT is applied to the studied system which can be considered as a low-cost prototype used for photovoltaic water pumping system and quick tracking of maximum power.

The studied system is modeled and simulated under the MATLAB environment, and obtained results by simulation are presented.

2. MODELING OF THE PROPOSED SYSTEM

In the case of a method speed drive system of an induction motor supplied by a PV generator, two types of stand-alone PV systems can be considered [2].

- A structure with two static converters.
- A single static converter structure.

In this paper, the second structure, which needs only one converter, has been used. In this case, the proposed system is represented in Figure 1. It consists of an induction motor fed by a photovoltaic generator through a three-phase voltage inverter controlled by the DTC technique.

2.1. Photovoltaic Array Modelling

2.1.1. One diode model

The equivalent circuit consists of a single diode for the phenomena of cell polarization and two resistors (series and shunt) for the losses is presented in Figure 2.

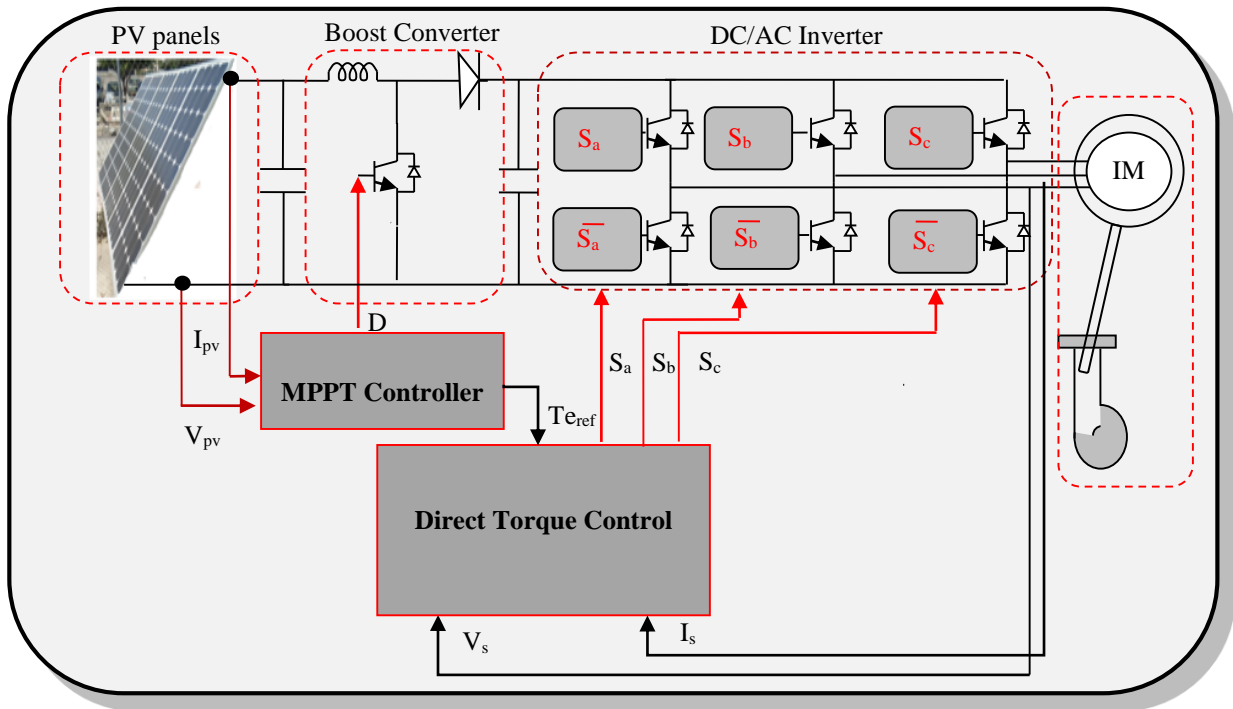


Fig.1. Proposed studied system

This model is given by the following Equation (1):

$$I_{pv} = I_{ph} - I_d - I_{Rsh} \tag{1}$$

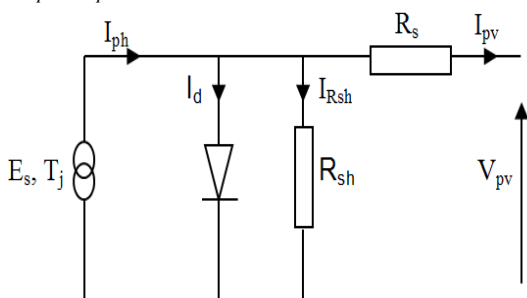


Fig. 2. Equivalent circuit (one diode model) [2]

This model is characterized by a very simple resolution. It requires only four parameters namely I_{sc} , V_{oc} , V_{mp} , and I_{mp} . The model is as follows [2]:

$$I_{pv} = I_{sc} \left\{ 1 - C_1 \left[\exp\left(\frac{V_{pv}}{C_2 \cdot V_{oc}}\right) - 1 \right] \right\} \tag{2}$$

$$C_2 = \frac{\left(\frac{V_m}{V_{oc}}\right) - 1}{\ln\left(1 - \frac{I_m}{I_{sc}}\right)} \tag{3}$$

$$C_1 = \left(1 - \frac{I_m}{I_{sc}}\right) \exp\left(-\frac{V_m}{C_2 \cdot V_{oc}}\right)$$

2.1.2 Two diode model

In this model, the two diodes represent the PN junction polarization phenomena. These diodes represent the recombination of the minority carriers which are located both at the surface of the material and within the volume of the material as in Figure 3.

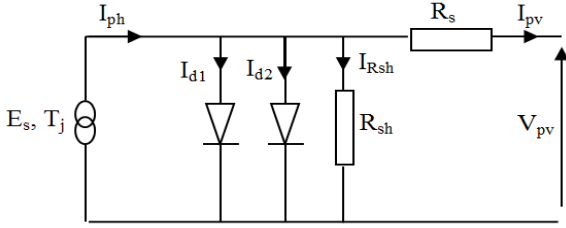


Fig. 3. The equivalent circuit for two diode model

The following equation is then obtained:

$$I_{pv} = I_{ph} - (I_{d1} + I_{d2}) - I_{Rsh} \tag{4}$$

With I_{ph} and I_{Rsh} maintaining the same expressions as above. For the recombination currents, we have:

$$\begin{cases} I_{d1} = I_{o1} \cdot \left[\exp\left(\frac{q \cdot (V_{pv} + R_s \cdot I_{pv})}{A \cdot N_s \cdot k \cdot T_j}\right) - 1 \right] \\ I_{d2} = I_{o2} \cdot \left[\exp\left(\frac{q \cdot (V_{pv} + R_s \cdot I_{pv})}{2 \cdot A \cdot N_s \cdot k \cdot T_j}\right) - 1 \right] \end{cases} \tag{5}$$

The saturation currents are written as follows;

$$\begin{cases} I_{o1} = P_4 \cdot T_j^3 \cdot \exp\left(\frac{-E_g}{k \cdot T_j}\right) \\ I_{o2} = P_5 \cdot T_j^3 \cdot \exp\left(\frac{-E_g}{2 \cdot k \cdot T_j}\right) \end{cases} \tag{6}$$

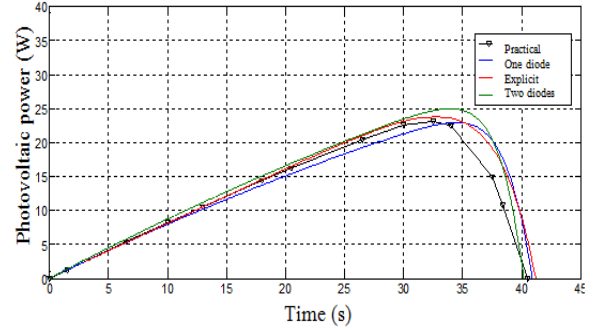
Where N_s is the number of cells in branched series, E_g represents the gap energy. The final equation of the model is written as:

$$I_{pv} = P_1 \cdot E_s \cdot \left[1 + P_2 \cdot (E_s - E_{sref}) + P_3 \cdot (T_j - T_{ref}) \right] \cdot \frac{(V_{pv} + R_s \cdot I_{pv})}{R_{sh}} \cdot P_{04} \cdot T_j^3 \cdot \exp\left(\frac{-E_g}{k \cdot T_j}\right) \cdot \left[\exp\left(\frac{q \cdot (V_{pv} + R_s \cdot I_{pv})}{A \cdot N_s \cdot k \cdot T_j}\right) - 1 \right] - P_{14} \cdot T_j^3 \cdot \exp\left(\frac{-E_g}{2 \cdot k \cdot T_j}\right) \cdot \left[\exp\left(\frac{q \cdot (V_{pv} + R_s \cdot I_{pv})}{2 \cdot A \cdot N_s \cdot k \cdot T_j}\right) - 1 \right] \tag{7}$$

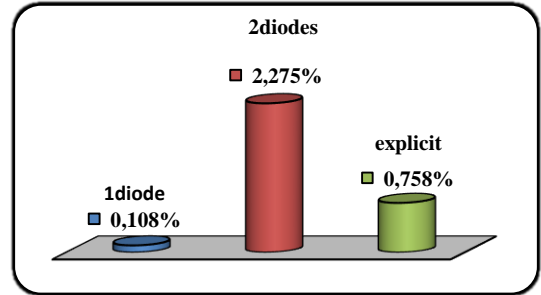
Validation has been made using PV panel Siemens SM110-24 as seen in Table1.

Parameters	Values
P_{mpp}	110W
I_{mpp}	3.15A
V_{mpp}	35V
I_{sc}	3.45A
V_{oc}	43.5V
α_{sc}	1.4mA/°C
β_{oc}	-152mV/°C

Results of power characteristics are obtained by different mathematical models and those obtained by experiment are presented in Figures 4-6. With: E_s solar irradiation (W/m²) and T_a ambient temperature (°C). It is noticed a good agreement between experimental and simulation characteristics especially in low and moderate irradiances which validates the mathematical model. The error on power is much greater for the two diode model. The one diode model results are closest to the experimental ones, therefore this model is adopted in current study.

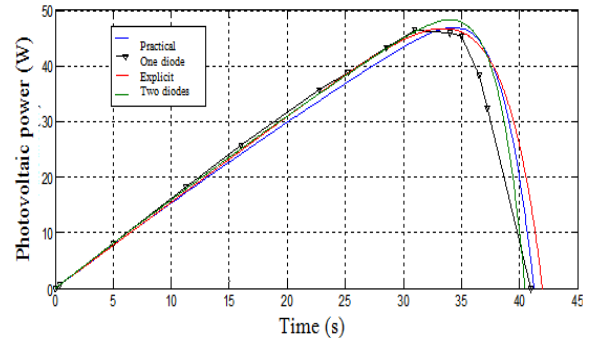


(a)

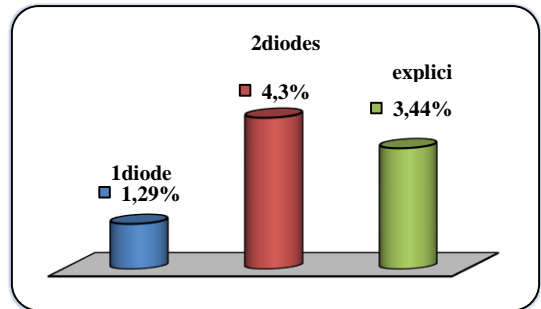


(b)

Fig. 4. Power characteristic at $E_s=244$ W/m², $T_a=24^\circ$ C, (a)Photovoltaic power, (b)Power error calculation

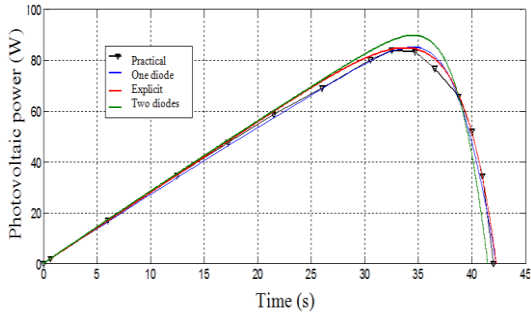


(a)

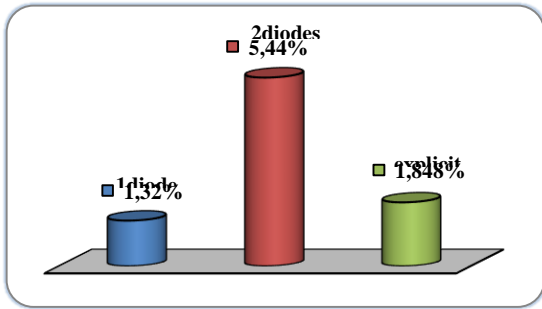


(b)

Fig. 5. Power characteristic at $E_s=460$ W/m², $T_a=29^\circ$ C, (a)Photovoltaic power, (b)Power error calculation



(a)



(b)

Fig. 6. Power characteristic at $E_s=856 \text{ W/m}^2$, $T_a=32^\circ\text{C}$, (a)Photovoltaic power, (b)Power error calculation

2. 2. MPPT Algorithm

Many methods have been developed to determine the MPPT control. In this paper, the P&O method is used due to its implementation simplicity in photovoltaic water pumping system. The flowchart of the P&O algorithm is given in Figure 7.

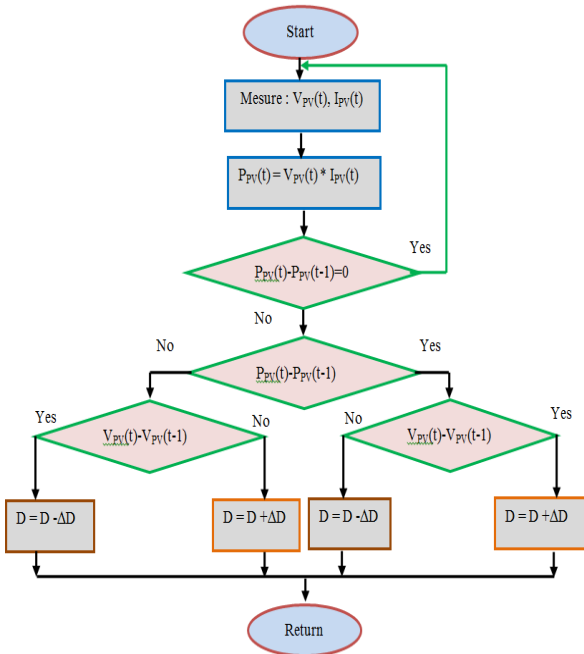


Fig. 7. Flowchart of the P&O MPPT algorithm

The panel voltage is deliberately perturbed, then the power is compared to the power obtained before to disturbance. Specifically, if the power panel is increased due to the disturbance, the following disturbance will be made in the same direction. If the power decreases, the new perturbation is made in the opposite direction.

2.1. Machine Modelling

An induction motor is modelled using voltage and flux equations, which are referred to as a general frame and are shown as follows:

Stator voltage equations:

$$\begin{cases} V_{S\alpha} = R_S I_{S\alpha} + \frac{d\Phi_{S\alpha}}{dt} \\ V_{S\beta} = R_S I_{S\beta} + \frac{d\Phi_{S\beta}}{dt} \end{cases} \quad (8)$$

where: $I_{S\alpha}$, $I_{S\beta}$ are for α , β stator currents respectively. $\Phi_{S\alpha}$, $\Phi_{S\beta}$ are for α , β stator flux respectively, R_S is the stator resistance.

$$\begin{cases} 0 = V_{R\alpha} = R_R I_{R\alpha} + \frac{d\Phi_{R\alpha}}{dt} + \frac{d\theta}{dt} \Phi_{R\beta} \\ 0 = V_{R\beta} = R_R I_{R\beta} + \frac{d\Phi_{R\beta}}{dt} - \frac{d\theta}{dt} \Phi_{R\alpha} \end{cases} \quad (9)$$

where: $I_{R\alpha}$, $I_{R\beta}$ are for α , β rotor current respectively, $\Phi_{R\alpha}$, $\Phi_{R\beta}$ are for α , β rotor flux respectively, R_r is the rotor resistance.

$$\begin{cases} \Phi_{S\alpha} = L_S I_{S\alpha} + L_m I_{R\alpha} \\ \Phi_{S\beta} = L_S I_{S\beta} + L_m I_{R\beta} \\ \Phi_{R\alpha} = L_R I_{R\alpha} + L_m I_{S\alpha} \\ \Phi_{R\beta} = L_R I_{R\beta} + L_m I_{S\beta} \end{cases} \quad (10)$$

Mechanical equations:

$$T_e - T_L = J_m \cdot \frac{d\omega_r}{dt} \quad (11)$$

$$T_e = P \times (\phi_{s\alpha} \times I_{s\beta} - \phi_{s\beta} \times I_{s\alpha})$$

where: T_e is the electromagnetic torque, T_L the load torque, J_m the inertia, P is the pole number and ω_r the rotor angular speed.

2. 3. Inverter Modelling

For each possible switching configuration, the output voltages can be represented in terms of space vector, according to the following equation:

$$V_s = V_{s\alpha} + jV_{s\beta} = \sqrt{\frac{2}{3}} \left[V_a + V_b \exp\left(j\frac{2\pi}{3}\right) + V_c \exp\left(j\frac{4\pi}{3}\right) \right] \quad (12)$$

where: V_a , V_b , and V_c are phase voltages.

2.4. Pumping System Modelling

The model of the power input (P) is given as [14]:

$$P(h, Q) = a(h).Q^3 + b(h).Q^2 + c(h).Q + d(h) \quad (13)$$

where: $a(h)$, $b(h)$, $c(h)$, $d(h)$ are the different coefficients:

$$a(h) = a_0 + a_1 h^1 + a_2 h^2 + a_3 h^3 \quad (14)$$

$$b(h) = b_0 + b_1 h^1 + b_2 h^2 + b_3 h^3 \quad (15)$$

$$c(h) = c_0 + c_1 h^1 + c_2 h^2 + c_3 h^3 \quad (16)$$

$$d(h) = d_0 + d_1 h^1 + d_2 h^2 + d_3 h^3 \quad (17)$$

where: $a_i, b_i, c_i,$ and d_i constants.
For $P > 0$, we have:

$$Q_k = Q_{k-1} - \frac{F(Q_{k-1})}{F'(Q_{k-1})} \quad (18)$$

where:

$$F(Q_{k-1}) = a Q_{k-1}^3 + b Q_{k-1}^2 + c Q_{k-1} + d - P_a \quad (19)$$

3. STUDIED SYSTEM CONTROL

Six non-zero voltage vectors and two zero-voltage vectors can be applied to the machine terminals. The stator flux can be estimated as [15]:

$$\phi_s(t) = \int_0^t (V_s - R_s i_s) dt \quad (20)$$

Since stator resistance $R_s i_s$ relatively small, $V_s \gg R_s i_s$,

$$\phi_s(t) = V_s T + \phi_s(0) \quad (21)$$

where $\phi_s(0)$ is the initial value of stator flux, T the sampling period. The stator voltage vector V_s is selected using Table 2, where signs errors E_T and E_ϕ are determined with a zero hysteresis band.

$$E_T = T_{e ref} - T_e \quad (22)$$

$$E_\phi = \phi_{s ref} - \phi_s \quad (23)$$

$$\phi_s = \sqrt{(\phi_{s\alpha})^2 + (\phi_{s\beta})^2} \quad (24)$$

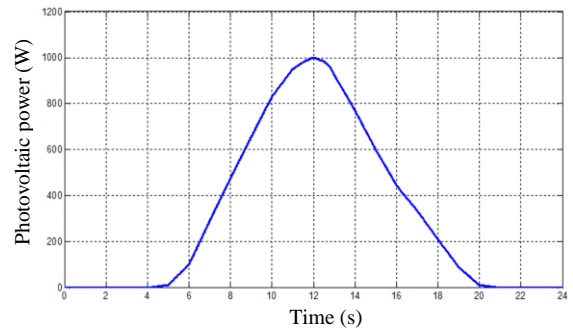
Table 2 provides the associated inverter switching states.

Table 2. Switching table for DTC

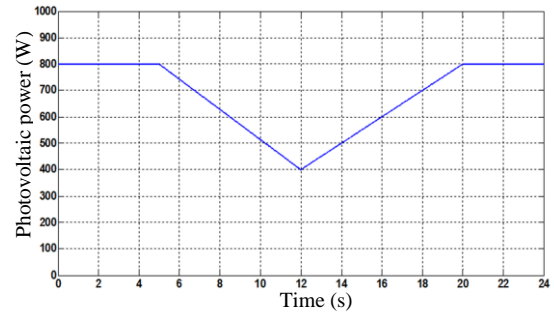
E_T	E_ϕ	N					
		1	2	3	4	5	6
1	1	V_2	V_3	V_4	V_5	V_6	V_1
	0	V_6	V_1	V_2	V_3	V_4	V_5
0	1	V_3	V_4	V_5	V_6	V_1	V_2
	0	V_5	V_6	V_1	V_2	V_3	V_4

4. SIMULATION RESULTS

A simulation of the proposed system has been carried out by means of MATLAB/Simulink. Two different solar irradiance variations in Figure 8 have been used for one-day profile and sudden variation. The sampling period of the system is about $T=100\mu s$. The obtained results are represented in Figures 9-11.



(a)



(b)

Fig. 8. Solar irradiance, (a) one day profile, (b) sudden variation

The stator flux in Figure 9 keeps its reference ($\Phi_{sref}=0.8$ Wb) during the two different irradiation profiles.

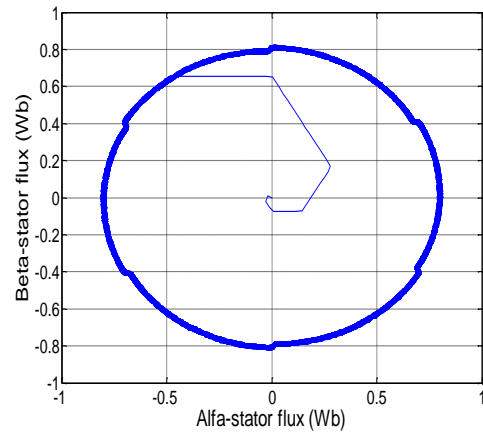


Fig. 9. Stator flux trajectory

It is noticed that the continuous power obtained at the output of the photovoltaic generator in Figure 10 (a) is in accordance with the solar irradiation profile. It reaches a maximum value at the maximum irradiation level. It can also be observed that the MPPT algorithm perfectly tracks and locates the point of maximum power for a given irradiance. This implies that the photovoltaic generator is operating at its optimal efficiency. The electromagnetic torque, which presents significant ripples in Figure 10 (b), follows the reference and takes the shape of the solar irradiance. This means that for high values of irradiance, the machine accelerates by increasing the water pumped volume.

The stator current in Figure 10 (c) follows the irradiance profile. It is noticed that the voltage DC bus remains constant and follows its reference within a small

range of variation without being affected by the change of solar irradiance in Figure 10 (d). The water flow rate in Figure 10 (e) changes with the intensity of the solar irradiation since the motor pump uses a continuously variable power, and therefore a variable speed. In

addition, with the introduction of MPPT algorithm, the mechanical speed Figure 11 (a) increases with the increase of the water flow in Figure 11 (b) during the observed period. The same remark can be made for the sudden variation profiles in Figures 11(b) and 11(c).

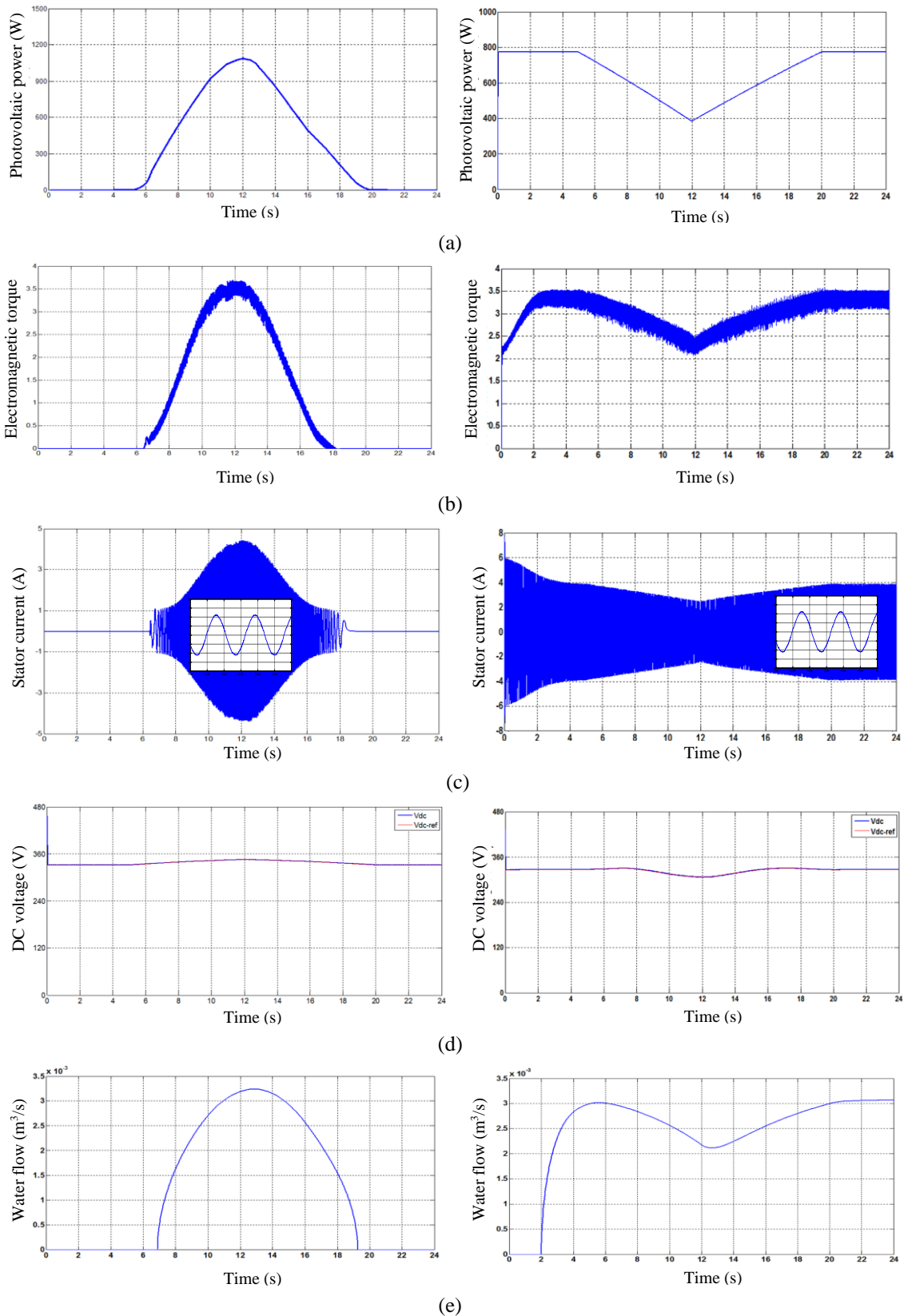


Fig. 10. System performances under two different solar irradiance (Left: under solar irradiation profile, Right under sudden variation profile) a) Photovoltaic power, b) Electromagnetic torque, c) Stator current, d) DC voltage variation with time, (e) Water flow

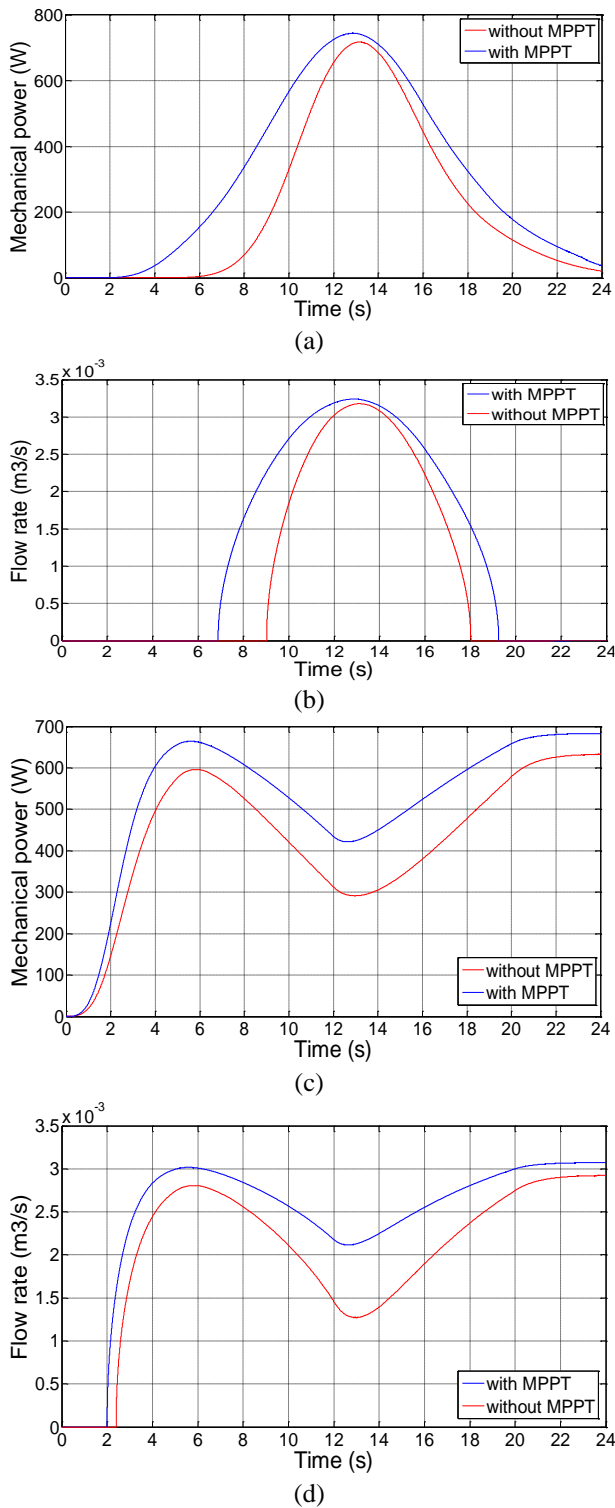


Fig.11. System performances with and without MPPT, (a) Mechanical power during a profile of one day, (b) Flow rate during a profile of one day, (c) Mechanical power during irradiance variation, (d) Flow rate during irradiance variation.

It is noticed that the mechanical power increases with the introduction of the MPPT, and thus the water flow increases. In addition, with the variation of irradiance, mechanical power and flow rate follow the variations with a marked improvement with the introduction of the MPPT.

6. CONCLUSION

Direct torque control of an induction generator supplied by a photovoltaic system has been proposed in this paper. The results have shown that the performances obtained are very attractive for the application of this control in photovoltaic system, especially in water pumping installations. Simulation results showed that the PV pumping system offers maximum pumping flow rate due to the MPPT (P&O method). The application of DTC in a photovoltaic pumping system maximizes power, which improves the total efficiency of the system. It was noticed that there is a lot of ripples in the torque; and it would be interesting to use a modulated hysteresis controller, which leads to an important reduction of the torque ripples. Besides, with the introduction of power optimization, the algorithm gives better tracking and allows us to improve the performance of the proposed system with a very high intake of water flow.

References

- [1] S. O. Amrouche, D. Rekioua, T. Rekioua, Overview of energy storage in renewable energy systems, Proceedings of 2015 IEEE International Renewable and Sustainable Energy Conference, IRSEC 2015, art. no. 7454988, (2016).
- [2] D. Rekioua, E. Matagne, Optimization of Photovoltaic Power Systems, Modelization, Simulation and Control, Edition Springer, Green Energy and Technology, 102, (2012).
- [3] M. S. Ebrahim, A.M. Sharaf, A.M. Atallah, and A.S. Emarah, An Efficient Controller for Standalone Hybrid-PV Powered System, Turkish Journal of Electromechanics & Energy 2(1), 9-15, (2017).
- [4] M. A. Ramli, S. Twaha, K. Ishaque, A. YAl-Turki, A review on maximum power point tracking for photovoltaic systems with and without shading conditions', Renewable and Sustainable Energy Reviews, 67, 144–159, (2017).
- [5] N. Karami, N. Moubayed, R. Outbib, General review, and classification of different MPPT Techniques, Renewable and Sustainable Energy Reviews, 68(1), 1-18, (2017).
- [6] A. R. Reisi, M. H. Moradi, S. Jamasb, Classification and comparison of maximum power point tracking techniques for photovoltaic system: a review, Renew. Sustainable Energy Rev. 19 (C), 433–443, (2013).
- [7] D. P. Hohm and M. E. Ropp, Comparative study of maximum power point tracking algorithms, Progress in Photovoltaics: Research and Applications, 11, 47-62, (2003).
- [8] V. Salas, E. Olias, A. Barrado, A. Lazaro, Review of The Maximum Power Point Tracking Algorithms for Stand-Alone Photovoltaic Systems, Solar Energy Materials & Sol. Cells, 90 (11), 1555–1578 (2006).
- [9] S. Necaibia, M. S. Kelaiaia, H. Labar, A. Necaibia, Implementation of an Improved Incremental Conductance MPPT Control Based Boost Converter in Photovoltaic Applications, International Journal of Emerging Electric Power Systems, 18 (4), 1-19, (2017).

- [10] R. Cakmak, I. H. Altas, A. M. Sharaf, Modeling of FLC-Incremental based MPPT using DC-DC boost converter for a standalone PV system, International Symposium on Innovations in Intelligent Systems and Applications, Trabzon, 1-5, (2012)
- [11] M. S. Ghayad, N. M. Badra, A. Y. Abdelaziz, A. M. Sharaf, M. A. Attia, A New efficient self-adjusting PSO algorithm to enhance reactive power response of VSC-HVDC system, Turkish Journal of Electromechanics & Energy, 5(1), 28-36, (2020).
- [12] S. Bensmail, D. Rekioua, H. Azzi, Study of hybrid photovoltaic/fuel cell system for stand-alone applications, International Journal of Hydrogen Energy, 40(39), 13820-13826, (2015).
- [13] M. R. Douiri, Particle swarm optimized neuro-fuzzy system for photovoltaic power forecasting model, Solar Energy, 91-104, (2019).
- [14] H. Hamdi, C.B. Regaya, A. Zaafouri, A sliding-neural network control of induction-motor-pump supplied by a photovoltaic generator, Protection and Control of Modern Power Systems, 5 (1), art. no. 1, (2020).
- [15] D. Rekioua, F. Zaouche, H. Hassani, T. Rekioua, S. Bacha, Modeling and fuzzy logic control of a stand-alone photovoltaic system with battery storage, Turkish Journal of Electromechanics & Energy, 4 (1), 11-17, (2019).
- [16] S. Abouda, F. Nolet, A. Chaari, N. Essoumbouli, Y. Koubaa, Direct Torque Control DTC of Induction Motor Used for Piloting a Centrifugal Pump Supplied by Photovoltaic Generator, International Journal of Electrical, Computer, and Communication Engineering, 7(8), 1110-1115, (2013).
- [17] T. Rekioua, D. Rekioua, Direct torque control strategy of permanent magnet synchronous machines 2003 IEEE Bologna PowerTech - Conference Proceedings, 2, art. no. 130466 , 861-866, (2003).
- [18] P. K. Behera, M. K. Behera, A. K. Sahoo, Comparative Analysis of Scalar & Vector Control of Induction Motor Through Modeling & Simulation, International Journal of Innovative Research, Electronics, Instrumentation, and Control Engineering, 2(4), 1340-1344, (2014).
- [19] Z. Mokrani, D. Rekioua, T. Rekioua, Control of Fuel Cells-Electric Vehicle Based on Direct Torque Control, Turkish Journal of Electromechanics & Energy, 3(2), 8-14, (2018).
- [20] S. J. Salehi, J. Siahbalaee, Loss minimization strategy under direct torque control method using matrix converter fed IPMS Motor, Journal of Electrical Engineering, 16 (2), 135-143, (2016).

Nomenclature

ANN	Neural networks algorithm
DTC	Direct Torque Control
FLC	Fuzzy logic controller
IG	Induction generator
IncCond	Conductance incremental algorithm
MPP	Maximum power point tracking
P&O	Perturb & Observe
SMC	Sliding mode controller
E_s	Solar irradiation (W/m^2)
$I_{s\alpha}, I_{s\beta}$	α, β stator current (A),
J_m	Mechanical inertia ($kg.m^2$),
L_R, L_S	Stator and rotor inductance (H),
L_m	Magnetizing inductance (H),
N_s	Number of cells in branched series,
P	Pole number
R_s	Stator resistance (Ω)
T_a	Ambient temperature ($^{\circ}C$),
T_e	Electromagnetic torque (N.m)
T_L	Load torque (N.m)
V_s	Voltage vector (V),
α, β	Concordia transformation components
$\Phi_{s\alpha}, \Phi_{s\beta}$	α, β stator flux respectively,
ω_r	Rotor angular speed (rad/s)

Biographies



Ahmed Mohammadi received his Master and PHD diploma from the University of Bejaia (Algeria). He is associate Professor at the Electrical Engineering Department-University of Bouira (Algeria) since 2015. His research activities have been devoted to several topics: photovoltaic systems, modelling, batteries and control in AC machines.

E-mail: mohammed_ahmed06@yahoo.fr



Djamilia Rekioua received the engineer degree in electrical engineering in 1987, the master's degree, in 1993, both from the Ecole Nationale Polytechnique, Algiers, Algeria, and the Ph.D. degree in 2002. Her current research interests include control of AC machines and electric drives, and renewable energies. She is Professor at the University of Bejaia (Algeria), head of the Team Renewable Energy in LTII Laboratory of the University of Bejaia.

E-mail address: dja_rekioua@yahoo.fr